

Syntheses and Structures of Mono- and Dinuclear Platinum Complexes of Pyrimidine-2-thiolate and Its 4-Methyl and 4,6-Dimethyl Derivatives

Osamu Asada, Keisuke Umakoshi,†* Kiyoshi Tsuge, Shingo Yabuuchi,† Yoichi Sasaki, and Masayoshi Onishi†

Division of Chemistry, Graduate School of Science, Hokkaido University, Kita-ku, Sapporo 060-0810

†Department of Applied Chemistry, Faculty of Engineering, Nagasaki University, Bunkyo-machi, Nagasaki 852-8521

(Received August 5, 2002)

The reaction of $K_2[PtCl_4]$ with pyrimidine-2-thiol (pymSH) was reinvestigated. Among the possible four isomers, the major product was the cis isomer of $[Pt^{III}_2Cl_2(pymS)_4]$ (**1**). The Pt(II) complex *cis*-$[Pt_2(pymS)_4]$ (**2**) was prepared by the addition of $NaOCH_3$ in the reaction mixture. The substitution of the axial Cl^- ligands of **1** with Br^- afforded the bromo complex $[Pt_2Br_2(pymS)_4]$ (**3**). While the reactions of $K_2[PtCl_4]$ with 4-methylpyrimidine-2-thiol hydrochloride (4-mpymSH·HCl) in the presence of $NaHCO_3$ gave a mixture of $[Pt_2Cl_2(4\text{-mpymS})_4]$ (**4**) and *trans*-$[Pt(4\text{-mpymS})_2]$ (**5**), the reaction with 4,6-dimethylpyrimidine-2-thiol (4,6-dmpymSH) gave only *trans*-$[Pt(4,6\text{-dmpymS})_2]$ (**7**). The preference of bis-chelate mononuclear complexes for these ligands may be explained by considering steric hindrance between the ligands in the dimer. The oxidation of **5** by Ce(IV) afforded *trans*-dichloro Pt(IV) complex, $[PtCl_2(4\text{-mpymS})_2]$ (**6**). The crystal structures of **1**, **3**, **6** and **7** were determined. The redox properties of **1** and **3** are also discussed.

Quadruply bridged dinuclear platinum complexes are known for a wide variety of bridging ligands such as acetate, sulfate, phosphate, pyrimidinethiolate, pyridinethiolates, diphosphonate, and dithiocarboxylates, where the bite distances of bridging ligands range from 2.2 to 3.1 Å.[1] Classification of the complexes by the bite distance of bridging ligands revealed the dependence of the oxidation state of platinum center on the bite distance. Thus the bridging ligands with the bite distance less than ca. 2.7 Å gave Pt(III) dimers, while those with the bite distances longer than ca. 2.7 Å afforded Pt(II) dimers. It is interesting to note that the distance of ca. 2.7 Å corresponds to the Pt-Pt bond length of the unbridged diplatinum(III) compounds.[2,3]

Pyridine-2-thiolate ligands (R-pyt) such as pyridine-2-thiolate (pyt), 4-methylpyridine-2-thiolate (4-mpyt) and 5-methylpyridine-2-thiolate (5-mpyt) exhibit the *border* bite distances (2.71–2.74 Å). Thus these ligands give the Pt(II) and Pt(III) dimers as stable forms depending on the conditions,[4] and the complexes show some unique properties. For example, the Pt(II) complexes abstract chlorine from chloroform to give $[Pt^{III}_2Cl_2(R\text{-pyt})_4]$. We have recently reported that such readiness of $[Pt^{II}_2(5\text{-mpyt})_4]$ toward oxidation is the driving force of the formation of the tetrasulfido-bridged dimer of the dinuclear Pt(III) complex, $[\{ClPt_2(5\text{-mpyt})_4\}_2S_4]$, in the reaction of $[Pt^{III}_2Cl_2(5\text{-mpyt})_4]$ with $(Pr_4N)_2WS_4$, where $(Pr_4N)_2WS_4$ behaves as a reducing agent.[5]

While extending the study on the reactivity of dinuclear Pt(III) complexes toward tetrathiometalate anions to pyrimidine-2-thiolate (pymS) complex, we encountered a few unexpected results. First, the geometrical isomer of $[Pt_2Cl_2(pymS)_4]$ is different from that reported previously. When two coordinating atoms of the bridging ligands are different, as in the case of pyrimidine-2-thiolates, four geometrical isomers are possible for the quadruply bridged complexes. Here we call such isomers "*cis*", "*trans*", "*3,1*", "*4,0*" isomers according to their structures, as illustrated in Chart 1. The dinuclear Pt(III) complexes of pyrimidine-2-thiolate, $[Pt_2X_2(pymS)_4]$ (X

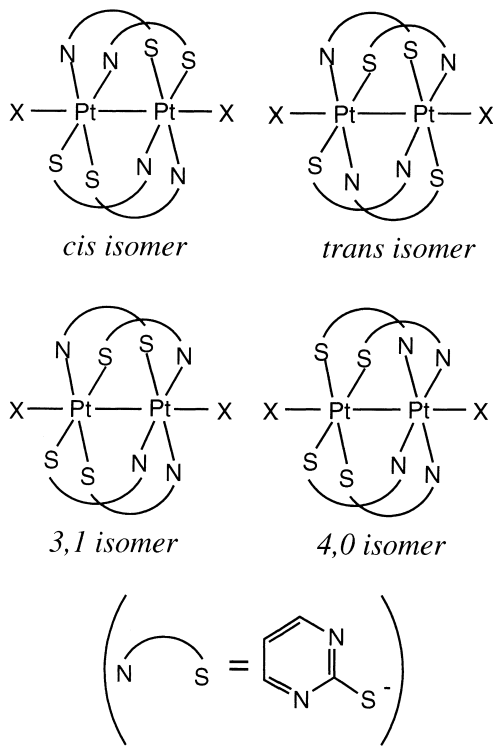

Chart 1.

= Cl, Br, I)[6,7] and $[Pt_2Cl(pymS)_5]$,[8] have been prepared by Goodgame and co-workers more than 10 years ago. In their reports, the iodo and bromo (not fully reported) complexes are "*cis* isomer" (each Pt atom takes cis configuration), while the chloro complex is "*3,1* isomer" (one of the Pt atoms is surrounded by three S atoms and one N atom, and the other Pt atom by one S atom and three N atoms). The complex that we prepared by the reported procedure turned out to be "*cis* isomer" instead of "*3,1* isomer" as was confirmed by ^{1}H NMR and X-ray structural determination. It could be that the isomer reported previously represented a minor product in the reaction mixture.

The second unexpected result is the ready formation of mononuclear complexes. In the reaction of $K_2[PtCl_4]$ with 4-methylpyrimidine-2-thiol (4-mpymSH) and 4,6-dimethylpyrimidine-2-thiolate (4,6-dmpymS), *trans*-$[Pt(4\text{-mpymS})_2]$ and *trans*-$[Pt(4,6\text{-dmpymS})_2]$, respectively, were obtained. It is interesting to find the mononuclear complexes in the reaction products, since no N-S chelate mononuclear Pt(II) complex has been structurally characterized for pyridine-2-thiolate and pyrimidine-2-thiolate so far. Mononuclear Pt(IV) complex, $[PtCl_2(4\text{-mpymS})_2]$ was also obtained by the oxidation of the crude product of the reaction of $K_2[PtCl_4]$ with 4-mpymSH.

Thus, the thorough investigation of the mono- and dinuclear Pt complexes of pymS- and related ligands is necessary in order to understand the reactivity of the dinuclear Pt complexes of these ligands towards tetrathiometalates and other reagents. In this paper, we summarize the preparation, structures and some properties of the mono- and dinuclear Pt complexes of pymS- and related pyrimidine-2-thiolate ligands.

Experimental

General. Dichloromethane was dried over calcium chloride and distilled under argon atmosphere. All other commercially available reagents were used as purchased.

UV-visible spectra were recorded on a Hitachi U3410 spectrophotometer at 20 °C. IR spectra were recorded on a Hitachi 270-50 infrared spectrophotometer. The ^{1}H NMR spectra were obtained at 270 MHz with a JEOL JNM-EX270 and at 300 MHz with a Varian Gemini300 spectrometers.

Cyclic voltammetry was performed with a Hokuto HA-301 potentiostat and a Hokuto HB-104 function generator equipped with a Yokokawa 3086 X-Y recorder. The working and the counter electrodes were a glassy-carbon disk and a platinum wire, respectively. Cyclic voltammograms were recorded at a scan rate of 50 mV/s. The sample solutions (ca. 0.4 mM) in 0.1 M $TBAPF_6$–CH_2Cl_2 ($TBAPF_6$ = tetra(*n*-butyl)ammonium hexafluorophosphate) were deoxygenated with a stream of argon. The reference electrode was Ag/AgCl and the half-wave potential of Fc^+/Fc ($E_{1/2}(Fc^{+/0})$ vs Ag/AgCl) was +0.47 V.

Preparation of the Complexes. ***cis*-$[Pt^{III}_2Cl_2(pymS)_4]$ (1).** This complex was prepared by a literature method reported for the preparation of "*3,1*-$[Pt^{III}_2Cl_2(pymS)_4]$".[7] Yield: 267 mg (91.4%) from 280 mg (0.67 mmol) of $K_2[PtCl_4]$ and 145 mg (1.29 mmol) of pyrimidine-2-thiol (pymSH). Anal. Calcd for $C_{16}H_{12}Cl_2N_8Pt_2S_4$: C, 21.22; H, 1.34; N, 12.37; Cl, 7.83; S, 14.16%. Found: C, 21.20; H, 1.50; N, 12.12; Cl, 7.26; S, 14.06%. UV-vis (CH_2Cl_2)/nm: 260 (ε 8.0×10^4 M^{-1} cm^{-1}), ca 290 (sh), 360 (4.7×10^3), 440 (1.7×10^3). ^{1}H NMR (CD_2Cl_2) δ 6.98 (dd, 1H, H_5), 8.46 (dd, 1H, H_4), 9.36 (dd, 1H, H_6).

***cis*-$[Pt^{II}_2(pymS)_4]$ (2). Method (a):** Pyrimidine-2-thiol (68 mg, 0.61 mmol) was dissolved into warmed methanol solution of $NaOCH_3$ (34 mg, 0.63 mmol/15 cm^3). To the methanol solution was added an aqueous solution of $K_2[PtCl_4]$ (50 mg, 0.12 mmol/1 cm^3) and the mixture was stirred with heating. After 15 min, the yellow solution changed to orange and yellow solid was separated. The reaction mixture was cooled to room temperature. The yellow solid was filtered, washed with diethyl ether, and then dried in vacuo. Yield 13 mg (26%).

Method (b): A methanolic solution of $NaOCH_3$ (256 mg, 4.73 mmol/90 cm^3) was added to an acetone solution of **1** (400 mg, 0.44 mmol/100 cm^3). The resulting yellow precipitate was filtered, washed with water and methanol, and then dried in vacuo. Yield 304 mg (83%). Anal. Calcd for $C_{16}H_{12}N_8Pt_2S_4$: C, 23.02; H, 1.45; N, 13.42; S, 15.36%. Found: C, 23.48; H, 1.57; N, 13.02; S, 15.09%. ^{1}H NMR (DMF-d_6) δ 7.10 (dd, 1H, H_5), 8.33 (dd, 1H, H_4), 9.05 (dd, 1H, H_6).

***cis*-$[Pt^{III}_2Br_2(pymS)_4]$ (3).** A methanolic solution of NaBr (300 mg, 2.92 mmol/10 cm^3) was added to a chloroform solution of **1** (104 mg, 0.11 mmol/50 cm^3). The mixture was stirred for 30 min at 20 °C. The orange suspension was filtered to remove NaCl and the filtrate was concentrated to ca. 10 cm^3. An addition of diethyl ether (20 cm^3) to the solution gave orange solid. The solid was filtered, washed with diethyl ether, and dried in vacuo. Yield 36 mg (32%). It was recrystallized from acetone. Anal. Calcd for $C_{16}H_{12}Br_2N_8Pt_2S_4 \cdot C_3H_6O$: C, 21.68; H, 1.72; N, 10.65; Br, 15.18, S, 12.19%. Found: C, 21.50; H, 1.69; N, 10.36; Br, 15.42; S, 12.26%. UV-vis (CH_2Cl_2)/nm: 265 (ε 8.5×10^4 M^{-1} cm^{-1}), 320 (2.5×10^4), 403 (3.1×10^3), 465 (4.4×10^3). ^{1}H NMR (CD_2Cl_2) δ 6.96 (dd, 1H, H_5), 8.46 (dd, 1H, H_4), 9.50 (dd, 1H, H_6).

$[Pt^{III}_2Cl_2(4\text{-mpymS})_4]$ (4) and *trans*-$[Pt^{II}(4\text{-mpymS})_2]$ (5). An aqueous solution of $NaHCO_3$ (86 mg, 1.02 mmol/30 cm^3) was added to a hot ethanol solution of 4-methylpyrimidine-2-thiol hydrochloride (4-mpymSH·HCl) (161 mg, 0.99 mmol/80 cm^3). To the above solution was added an aqueous solution of $K_2[PtCl_4]$ (210 mg, 0.51 mmol/5 cm^3), and the mixture was refluxed for 1 h. Orange solid was filtered, washed with diethyl ether, and dried in vacuo. Yield 180 mg. The solid was then dissolved into dichloromethane (350 cm^3) for the purification. Yellow needle crystals, **5**, appeared after reduction of the solution volume by rotary evaporator. They were separated from the solution by filtration, washed with diethyl ether, and dried in vacuo. Yield 36 mg. Anal. Calcd for $C_{10}H_{10}N_4PtS_2$ (**5**): C, 26.97; H, 2.26; N, 12.58; S, 14.40%. Found: C, 26.84; H, 2.14; N, 12.64; S, 14.24%. ^{1}H NMR ($CDCl_3$) δ 2.22 (s, 3H, Me), 6.71 (d, 1H, H_5), 8.31 (d, 1H, H_6). FABMS: *m*/*z* 446 ($[M + H]^+$). The filtrate separated from the yellow crystals contains **4**. The filtrate was slowly evaporated under air. Orange micro crystals were filtered, washed with diethyl ether, and dried in vacuo. Yield 49 mg. Anal. Calcd for $C_{20}H_{20}Cl_2N_8Pt_2S_4$ (**4**): C, 24.98; H, 2.10; N, 11.65; Cl, 7.37; S, 13.33%. Found: C, 24.41; H, 1.93; N, 11.33; Cl, 7.73; S, 12.99%. UV-vis ($CHCl_3$)/nm: 262 (ε 7.4×10^4 M^{-1} cm^{-1}), 288 sh (3.0×10^4), 358 sh (3.9×10^3), 400 sh (2.0×10^3), 437 (1.6×10^3). ^{1}H NMR (CD_2Cl_2)/ppm: δ 2.42 (s, 3H, Me), 6.80 (d, 1H, H_5), 9.13 (d, 1H, H_6). FABMS: *m*/*z* 962 ($[M]^+$), 925 ($[M - Cl]^+$), 891 ($[M + H-2Cl]^+$).

***trans*-$[Pt^{IV}Cl_2(4\text{-mpymS})_2]$ (6).** To a dichloromethane solution of $[Pt(4\text{-mpymS})_2]$ **5** (57 mg, 0.13 mmol/130 cm^3) was added a methanol solution of KCl (20 mg, 0.26 mmol/50 cm^3) and then a methanol solution of $(NH_4)_2Ce(NO_3)_6$ (145 mg, 0.26 mmol/12 cm^3) with stirring. After stirring for 15 min at room temperature, the solvent was removed. The resulting orange solid was extract-

Table 1. Crystallographic Data and Experimental Details for $[Pt_2Cl_2(pymS)_4]\cdot CH_3CN$ (**1**·CH_3CN), $[Pt_2Br_2(pymS)_4]\cdot CHCl_3$ (**3**·$CHCl_3$), $[PtCl_2(4\text{-}mpymS)_2]$ (**6**) and $[Pt(4,6\text{-}dmpymS)_2]$ (**7**)

	1·CH_3CN	**3**·$CHCl_3$	**6**	**7**
Empirical formula	$C_{18}H_{15}Cl_2N_9Pt_2S_4$	$C_{17}H_{13}Br_2Cl_3N_8Pt_2S_4$	$C_{10}H_{10}Cl_2N_4PtS_2$	$C_{12}H_{14}N_4PtS_2$
M	946.70	1113.93	516.33	473.48
Crystal system	Monoclinic	Monoclinic	Orthorhombic	Monoclinic
Space group	*Cc*	$P2_1/a$	*Pbca*	*C*2/*c*
a/Å	11.724(2)	10.407(2)	12.615(1)	15.948(8)
b/Å	27.593(3)	20.395(2)	15.685(1)	13.009(2)
c/Å	9.820(2)	13.324(2)	7.373(1)	6.9057(6)
β/°	126.48(1)	93.50(1)	90	104.732(2)
V/Å^3	2554(1)	2822.6(7)	1458.8(3)	1385.6(7)
Z	4	4	4	4
T/K	296	296	296	123
Cryst size/mm	0.80 × 0.20 × 0.10	0.80 × 0.20 × 0.10	0.70 × 0.50 × 0.20	0.30 × 0.10 × 0.01
μ/mm^{-1}	11.46	13.31	10.22	10.38
T_{min}, T_{max}	0.673, 0.997	0.534, 0.999	0.511, 0.998	0.546, 0.901
No. reflections measured	3924	8548	2124	1445
No. reflections observed	3554	5773	1230	1192
R(int.)	0.038	0.033		0.025
R[a)]	0.021	0.037	0.028	0.028
R_w[b)]	0.019	0.024	0.022	0.039
GOF[c)]	1.51	1.69	2.78	2.22
$\Delta\rho_{max}$, $\Delta\rho_{min}$/e Å^{-3}	1.13, −0.52	1.46, −1.36	1.99, −0.91	1.63, −1.13

a) $R = \Sigma||F_o| - |F_c||/\Sigma|F_o|$. b) $R_w = [\Sigma w(|F_o| - |F_c|)^2/\Sigma w|F_o|^2]^{1/2}$; $w^{-1} = \sigma^2(|F_o|) + p|F_o|^2$ ($p = 2 \times 10^{-5}$ for **1**·CH_3CN, 4×10^{-6} for **3**·$CHCl_3$, **6** and **7**). c) The goodness of fit is defined as $[w(|F_o| - |F_c|)^2/(n_o\text{-}n_v)]^{1/2}$, where n_o and n_v denotes the numbers of data and variables, respectively.

ed with chloroform, and the orange solution was concentrated to dryness to give crude residue (23 mg, 34%). The solid was recrystallized from chloroform. Yield 8 mg (11%). Anal. Calcd for $C_{10}H_{10}Cl_2N_4PtS_2$: C, 23.26; H, 1.95; N, 10.85; Cl, 13.73; S, 12.42%. Found: C, 23.15; H, 1.83; N, 11.02; Cl, 13.50; S, 12.21%. ^{1}H NMR ($CDCl_3$) δ 2.55 (s, 3H, Me), 6.92 (d, 1H, H_5), 8.54 (d, 1H, H_6).

***trans*-[Pt^{II}(4,6-dmpymS)$_2$] (7).** An aqueous solution of $K_2[PtCl_4]$ (210 mg, 0.5 mmol/5 cm^3) was added to a hot aqueous solution of 4,6-dimethylpyrimidine-2-thiol (4,6-dmpymSH) (140 mg, 1.0 mmol/40 cm^3). The mixture was refluxed for 6 h. The resulting orange precipitate was filtered, washed with water, and then dried in vacuo. Yield 210 mg (88.7%). Anal. Calcd for $C_{12}H_{14}N_4PtS_2$: C, 30.44; H, 2.98; N, 11.83; S, 13.54%. Found: C, 30.35; H, 2.88; N, 11.75; S, 13.09%. ^{1}H NMR ($CDCl_3$) δ 2.15 (s, 3H, 4-Me), 2.40 (s, 3H, 6-Me), 6.56 (s, 1H, H_5).

Reaction of 4 with Ce(IV). An oxidation was attempted similarly to that of **5** by using **4** (149 mg, 0.15 mmol), KCl (24 mg, 0.32 mmol) and $(NH_4)_2Ce(NO_3)_6$ (169 mg, 0.31 mmol). After recrystallization from dichloromethane, **4** was recovered (87 mg (58%)), as confirmed by the FAB mass and ^{1}H NMR spectra.

X-ray Structural Determinations. A summary of pertinent crystallographic data and experimental details for complexes **1**, **3** , **6** and **7** is shown in Table 1. Crystals of **1**·CH_3CN, **3**·$CHCl_3$, **6** and **7** suitable for X-ray structural analysis were obtained by recrystallization from CH_3CN, $CHCl_3$, $CHCl_3$, and hot $(CH_3)_2SO$, respectively. The crystals of the former two complexes (**1**·CH_3CN and **3**·$CHCl_3$) were sealed in a thin-walled glass capillary, while those of the latter two (**6** and **7**) were mounted on a glass fiber. Intensity data were collected on a Rigaku AFC-5R diffractometer using graphite-monochromated Mo Kα ($\lambda = 0.71069$ Å) radiation at 296 K for **1**·CH_3CN, **3**·$CHCl_3$ and **6**. The unit cell parameters were obtained by least-squares refinement of 25 reflections ($25 \leq 2\theta \leq 30°$). The intensities of three standard reflections, monitored after every 150 reflections, showed no appreciable decay during the data collection. The data were corrected for Lorentz and polarization effects. An empirical absorption correction based on azimuthal scans of three reflections was applied.[9] For **7**, intensity data were collected on a Mercury CCD area detector coupled with a Rigaku AFC8S diffractometer using graphite-monochromated Mo Kα ($\lambda = 0.71069$ Å) radiation at 123 K. Final cell parameters were obtained from a least-squares analysis of reflections with $I > 10\sigma(I)$. Data were collected in 0.5° oscillations (in ω) with 60.0 s exposures (in two 30.0 s repeats to allow dezingering). Sweeps of data were done using ω oscillations from −76.0 to 104.0° at $\chi = 45.0°$ and $\phi = 0.0°$ and from −16.0 to 44.0° at $\chi = 45.0°$ and $\phi = 90.0°$. The crystal to detector distance was 40.5 mm, and the detector swing angle was 14°. The data were corrected for Lorentz and polarization effects. An empirical absorption correction was applied.[10]

The crystal structures of **1**·CH_3CN and **3**·$CHCl_3$ were solved by heavy-atom method by using DIRDIF94.[11] Those of **6** and **7** were solved by direct method (SIR92 for **6**[12] and MITHRIL90 for **7**[13]). The positional and thermal parameters of non-H atoms were refined anisotropically by the full-matrix least-squares method. H atoms were included at calculated positions with fixed displacement parameters (1.2 times the displacement parameters of the host atom). All calculations were performed using teXsan.[14] Listings of the selected bond distances and angles are summarized in Tables 2 and 3.

X-ray crystallographic files in CIF format for **1**·CH_3CN, **3**·$CHCl_3$, **6**, and **7** have been deposited at the CCDC, 12 Union Road, Cambridge CB2 1EZ, UK and copies can be obtained on request, free of charge, by quoting the publication citation and the

Table 2. Selected Bond Distances (Å) and Angles (°) for **1**·CH_3CN (X = Cl) and **3**·$CHCl_3$ (X = Br)

	1·CH_3CN	**3**·$CHCl_3$
Pt1–Pt2	2.5320(5)	2.5384(6)
Pt1–X1	2.427(2)	2.5667(9)
Pt1–S1	2.306(2)	2.303(2)
Pt1–S2	2.302(2)	2.304(2)
Pt1–N31	2.104(6)	2.122(6)
Pt1–N41	2.105(6)	2.109(5)
Pt2–X2	2.466(2)	2.5830(9)
Pt2–S3	2.308(2)	2.303(2)
Pt2–S4	2.296(2)	2.305(2)
Pt2–N11	2.091(6)	2.117(6)
Pt2–N21	2.117(6)	2.110(6)
S1···N11	2.719(6)	2.700(6)
S2···N21	2.707(5)	2.714(6)
S3···N31	2.704(4)	2.713(6)
S4···N41	2.715(5)	2.721(6)
Pt2–Pt1–X1	174.00(6)	174.31(2)
Pt2–Pt1–S1	89.96(5)	89.17(5)
Pt2–Pt1–S2	89.83(5)	90.18(5)
Pt2–Pt1–N31	89.7(2)	90.3(2)
Pt2–Pt1–N41	91.2(2)	89.6(2)
X1–Pt1–S1	87.67(7)	85.79(5)
X1–Pt1–S2	84.68(7)	87.25(5)
X1–Pt1–N31	92.8(2)	94.8(2)
X1–Pt1–N41	94.3(2)	93.1(2)
S1–Pt1–S2	90.40(7)	90.82(7)
S1–Pt1–N31	178.8(2)	179.1(2)
S1–Pt1–N41	91.2(2)	90.3(2)
S2–Pt1–N31	90.7(2)	89.9(2)
S2–Pt1–N41	178.1(2)	178.9(2)
N31–Pt1–N41	87.7(2)	89.0(2)
Pt1–Pt2–X2	175.23(5)	174.63(3)
Pt1–Pt2–S3	89.82(5)	89.54(5)
Pt1–Pt2–S4	89.89(5)	90.09(5)
Pt1–Pt2–N11	90.5(2)	89.5(2)
Pt1–Pt2–N21	90.0(2)	89.8(2)
X2–Pt2–S3	85.95(7)	89.11(5)
X2–Pt2–S4	88.00(7)	84.71(5)
X2–Pt2–N11	93.7(2)	91.9(2)
X2–Pt2–N21	92.2(2)	95.4(2)
S3–Pt2–S4	91.12(7)	89.80(8)
S3–Pt2–N11	179.5(2)	178.5(2)
S3–Pt2–N21	90.0(2)	90.4(2)
S4–Pt2–N11	89.2(2)	91.4(2)
S4–Pt2–N21	178.8(2)	179.8(2)
N11–Pt2–N21	89.6(2)	88.5(2)
S1–Pt1–Pt2–N11	24.3(2)	27.0(2)
S2–Pt1–Pt2–N21	25.0(2)	24.7(2)
N31–Pt1–Pt2–S3	25.7(2)	25.1(2)
N41–Pt1–Pt2–S4	22.2(2)	25.9(2)

deposition numbers 185252–185255.

Results and Discussion

The pymS Complexes. The dichloro complex, $[Pt_2Cl_2(pymS)_4]$, was prepared by the literature method reported for the preparation of "*3,1* isomer".[7] Orange-red precipitate was obtained in more than 90% yield. The ^1H NMR spectrum of the unpurified precipitate exhibits signals corresponding to the authentic *cis* isomer (confirmed by X-ray analysis, *vide infra*). The signals were superimposed with those of other species in relatively small intensities (Fig. 1). The superimposed signals may correspond to the "*3,1*" isomer, since the H_6 proton splits into 3 signals in the 1:2:1 ratio. After recrystallization from an appropriate organic solvent such as $CHCl_3$, CH_2Cl_2 or CH_3CN, pure *cis* isomer was obtained as a major product.

Table 3. Selected Bond Distances (Å) and Angles (°) for **6** and **7**

	6	**7**
Pt1-Cl1	2.316(2)	
Pt1-S1	2.403(2)	2.344(2)
Pt1-N13	2.038(5)	2.006(4)
Cl1-Pt1-S1	89.49(6)	
Cl1-Pt1-N13	89.9(2)	
S1-Pt1-N13	68.4(1)	69.8(1)

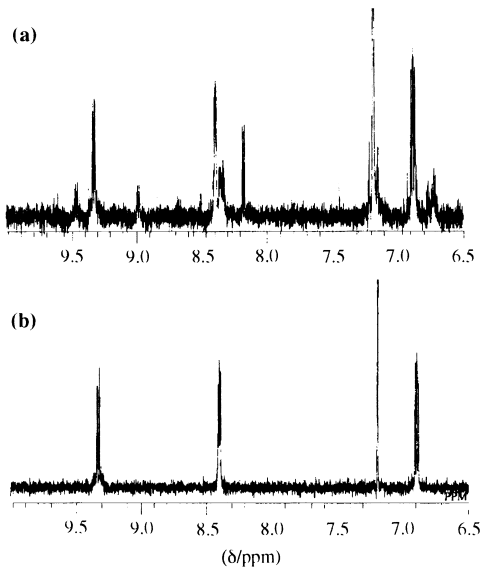

Fig. 1. ^1H NMR spectra (in $CDCl_3$) of the precipitate obtained by the reaction of $K_2[PtCl_4]$ with pyrimidine-2-thiol (a) and the recrystallized *cis*-$[Pt_2Cl_2(pymS)_4]$ (b).

The dimeric Pt(II) complex, *cis*-$[Pt_2(pymS)_4]$ (**2**), can be obtained directly by the reaction of $K_2[PtCl_4]$ with pyrimidine-2-thiol in the presence of NaOMe (method a). It can also be obtained by the reduction of the *cis* isomer of trivalent dichloro complex (method b) in much higher yield, thus suggesting the *cis* configuration of the Pt(II) dimer. In both cases, sodium methoxide acts as a reducing agent.

The two axial Cl^- ligands of Pt(III) dimer **1** can be substituted with bromide ions to give dibromo complex. The axial ligand substitution reaction is common to the dinuclear Pt(III) complexes having quadruply bridged structure.[1]

The 4-mpymS Complexes. Unlike the case of pyrimidine-2-thiol, the reaction of $K_2[PtCl_4]$ with 4-methylpyrimi-

dine-2-thiol afforded not only a dinuclear Pt(III) complex $[Pt_2Cl_2(4\text{-mpymS})_4]$ (**4**) but also a mononuclear Pt(II) complex *trans*-$[Pt(4\text{-mpymS})_2]$ (**5**) as a mixture. An attempt was made to oxidize the mixture in order to obtain a pure dinuclear Pt(III) complex, since the Pt(II) species were initially thought to be a dimer. A mixture of dinuclear Pt(III) complex and mononuclear Pt(IV) complex was obtained, however.

A pure sample of **4** as well as the mononuclear Pt(II) species **5** was obtained by recrystallization of the mixture from dichloromethane. The solubility of the dimeric Pt(III) complex is slightly higher among the two. The ^{1}H NMR spectrum of recrystallized dinuclear Pt(III) complex **4** exhibits one methyl signal, indicating the existence of only one isomer either *cis* or *trans* configuration, and the possibility of "*3,1*" isomer is excluded. Further identification of the geometrical isomers was not possible by spectroscopic measurements. Although it is difficult to measure the ^{1}H NMR spectrum of the recrystallized yellow mononuclear Pt(II) complex, **5**, owing to its low solubility for common deuterated solvents, that of the crude reaction product containing **4** and **5** can be measured. In that spectrum, **5** shows a set of signals at 2.22 (Me), 6.71 (H_5) and 8.31 ppm (H_6), indicating a single symmetrical structure, either *cis* or *trans*. The FAB mass spectrum of **5** is consistent with the monomeric structure.

The oxidation of **5** by two equivalents of Ce(IV) afforded a mixture of mononuclear Pt(IV) complex $[PtCl_2(4\text{-mpymS})_2]$ (**6**) and small amount of unidentified complex, the latter being removed by recrystallization of the mixture from $CHCl_3$. It is noteworthy that the use of the equivalent amount of Ce(IV) for the oxidation of **5** gave the 1:1 mixture of **5** and **6**. Pt(III) dimer **4** was not observed at all in the ^{1}H NMR spectrum of the reaction product. On the other hand, oxidation of **4** did not proceed in the reaction with Ce(IV). Such results indicate that the Pt(III) lantern structure is resistant towards oxidation, which would lead to the formation of Pt–Pt double bond or to the degradation of the dimer unit to give mononuclear Pt(IV) species.

$$[Pt^{II}(4\text{-mpymS})_2] \xrightarrow{Ce^{IV}} [Pt^{IV}Cl_2(4\text{-mpymS})_2] \quad (1)$$

$$[Pt^{III}_2Cl_2(4\text{-mpymS})_4] \xrightarrow{Ce^{IV}} \textit{no reaction} \quad (2)$$

The structure of Pt(IV) complex **6** was confirmed by X-ray analysis (vide infra). To our knowledge, pyrimidine-2-thiolates or pyridine-2-thiolates having no substituents at 6-position (*ortho* position to the coordinating N atom) have never been found as chelate ligands in the square planar Pt(II) or octahedral Pt(IV) monomer.[15] For these non-substituted ligands, the formation of the quadruply bridged Pt(II) or Pt(III) dimer seems to be a more favourable process. The only exceptions are $[NBu_4][Pt(C_6F_5)_2(pyt)Br_2]$ and $[Pt(C_6F_5)_2(pyt)(CN\text{-}t\text{-}C_4H_9)Br]$.[16] Pyrimidine-2-thiolates have two N atoms at 1 and 3-positions, which can form bridge or chelate with S atom at 2-position. In the reaction of $K_2[PtCl_4]$ with 4-mpymSH, the coordination of S atom to Pt atom is expected to take place first, since the affinity of S atom toward Pt atom is higher than that of N atom. If the second coordination takes place at the N1 atom, it leads to the formation of the dinuclear complex. However, if the second coordination proceeds at N3 atom, the steric repulsion between methyl groups of 4-mpymS ligands may prevent the formation of any isomer of the dinuclear complex, and as a consequence, it may lead to the formation of the bischelate mononuclear complex. Thus a mixture of dinuclear Pt(III) complex and mononuclear Pt(II) complex was obtained in the reaction of $K_2[PtCl_4]$ with 4-mpymSH.

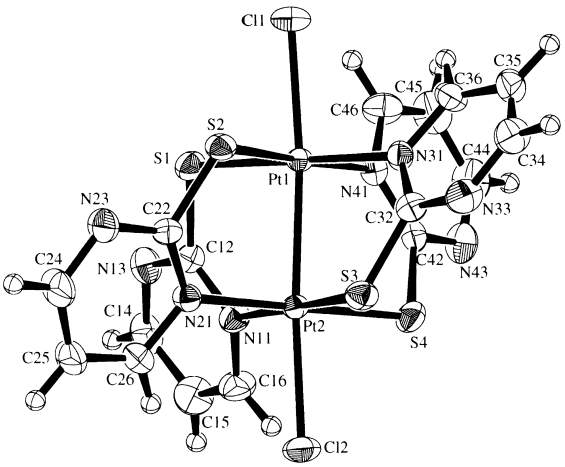

Fig. 2. ORTEP drawing of *cis*-$[Pt_2Cl_2(pymS)_4]$ **1** with the atomic labeling scheme (50% probability ellipsoids).

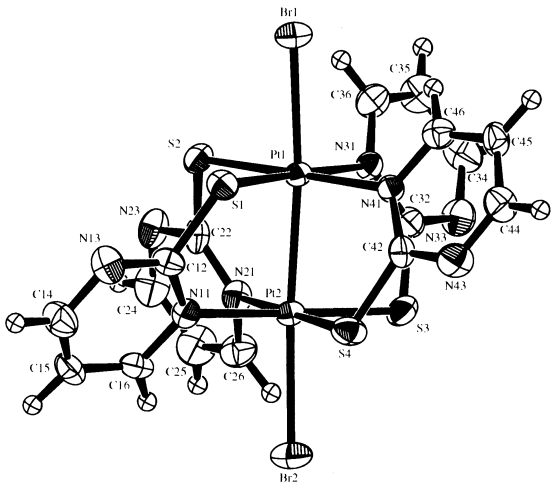

Fig. 3. Molecular structure of *cis*-$[Pt_2Br_2(pymS)_4]$ **3** with the atomic labeling scheme (50% probability ellipsoids).

The 4,6-dmpymS Complex. With the doubly methyl-substituted ligand, 4,6-dmpymS$^-$, the mononuclear Pt(II) complex was the only product. The ^{1}H NMR spectrum of **7**, showing a set of methyl signals at 2.15 and 2.40 ppm corresponding to 4 and 6 positions, respectively, indicates a symmetrical structure, either *trans* or *cis*. Among them the *cis* configuration is unlikely, due to steric repulsion of the methyl groups. The *trans* configuration was eventually confirmed by the X-ray structural analysis.

Structures of *cis*-$[Pt_2Cl_2(pymS)_4]$ (1), *cis*-$[Pt_2Br_2(pymS)_4]$ (3), *trans*(Cl)*trans*(N)*trans*(S)-$[PtCl_2(4\text{-mpymS})_2]$ (6) and *trans*-$[Pt(4,6\text{-dmpymS})_2]$ (7). The molecular structures of **1** and **3** are shown in Fig. 2 and 3, respectively. The structures of **1** and **3** are very similar to each other and also to that of iodo

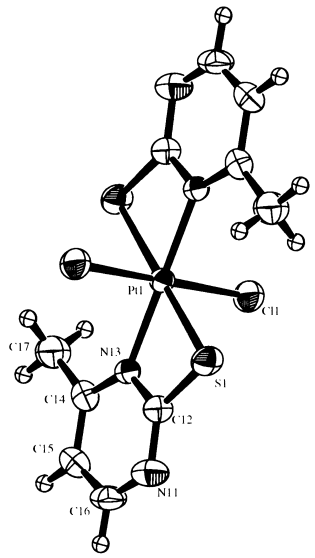

Fig. 4. ORTEP drawing of *trans*-[$PtCl_2$(4-mpymS)$_2$] **6** with the atomic labeling scheme (50% probability ellipsoids).

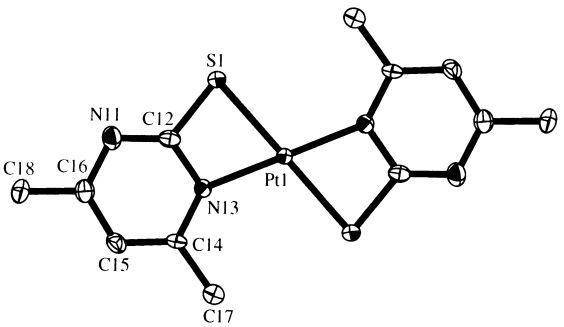

Fig. 5. ORTEP drawing of *trans*-[Pt(4,6-dmpymS)$_2$] **7** with the atomic labeling scheme (50% probability ellipsoids).

complex [Pt_2I_2(pymS)$_4$].[6] These two complexes have approximate C_{2h} symmetry. The square-planar PtS_2N_2 coordination sphere has a *cis* configuration. The two coordination spheres twist toward each other around the Pt–Pt axis, the average N–Pt–Pt–S torsion angles in **1** and **3** being 24.3° and 25.7°, respectively. The bite distance (the distance between the two donor atoms within a ligand; in this case, it is corresponding to the N···S distance) of pyrimidine-2-thiolate ligand is almost constant at 2.71 Å in the series of the Pt(III) dimers [Pt_2X_2(pymS)$_4$] (X = Cl, Br, I). Thus the twist angle should decrease as the Pt-Pt distance (X = Cl, 2.5320(5); X = Br, 2.5384(6); X = I, 2.554(1) Å) approaches to the bite distance. The order of the average twist angle (X = Cl (24.3°) < X = Br (25.7°) < X = I (ca 26°), is opposite, however. The difference in the Pt–Pt distance is so small that the influences of other factors such as Pt–S and Pt–N distances and bond angles to the twist angles become comparable. The tilt angles of axial ligand, Pt-Pt-X, in [Pt_2X_2(pymS)$_4$] are also very similar (X = Cl, av. 174.62°; X = Br, av. 174.47°; X = I, av 173.2°), indicating that the extent of the steric hindrance of pyrimidine rings toward axial ligands are also comparable by compensating the increase of Pt–X distances (X = Cl (av. 2.447 Å) < X = Br (av. 2.5749 Å) < X = I (2.774 Å)) (ionic radii of Cl^-, Br^-, and I^- are 1.81, 1.96, and 2.20 Å, respectively).[17] It is noteworthy that the Pt–Pt distance in **1** is the same as that in [Pt_2Cl_2(pyt)$_4$] (pyt = pyridine-2-thiolate; Pt–Pt = 2.532(1) Å; bite distance = 2.71 Å)[4] and is slightly longer than that in "*3*,*1*" isomer of [Pt_2Cl_2(pymS)$_4$] (2.518(1) Å).[7]

The molecular structure of **6** is shown in Fig. 4. The Pt atom lies on an inversion center and has a distorted octahedral geometry. The platinum atom is surrounded by two Cl, two N and two S atoms having *trans*(Cl)*trans*(N)*trans*(S) configuration. The (N13–Pt1–S1) angle is very small (68.4(1)°). The chelate coordination mode of the heterocyclic thiolates has been found for other transition metal complexes, but is rarely seen for divalent and tetravalent group 10 metal complexes.[15] The structural parameters of **6** (Pt1–S1, 2.403(2); Pt1–N13, 2.038(5) Å; S1-Pt1-N13, 68.4(1)°) can be compared with those of [Pd(4,6-dmpymS)$_2$] (4,6-dmpymS = 4,6-dimethylpyrimidine-2-thiolate: Pd–S, 2.341(1) Å; Pd–N, 2.016(3) Å; S–Pd–N, 70.2(1)°),[18] [NBu_4][Pt(C_6F_5)$_2$(pyt)Br_2] (Pt–S, 2.361(2) Å; Pt–N, 2.079(6) Å; S–Pt–N, 68.22(18)°).[16] The Pt-S and Pt-N distances in **6** are significantly shorter than those in [Pd(4,6-dmpymS)$_2$], [NBu_4][Pt(C_6F_5)$_2$(pyt)Br_2] and **7** (vide infra).

The X-ray structural analysis of **7** disclosed that the square-planar platinum(II) ion is coordinated by two 4,6-dmpymS ligands in a *trans* configuration (Fig. 5). The 4,6-dmpymS ligands also act as chelate ligands. The (S1–Pt1–N13 angle, 69.8(1)°), Pt1–S1 (2.344(2) Å) and Pt1–N13 (2.006(4) Å) distances are comparable to those in [Pd(4,6-dmpymS)$_2$][18] and [NBu_4][Pt(C_6F_5)$_2$(pyt)Br_2].[16] Since the Pt atom lies at the origin (inversion center) in the *C*2/*c* space group, the complex stacks in parallel along the c axis with Pt···Pt separation of 3.45 Å. The structure of **7** is isomorphous with that of [Pd(4,6-dmpymS)$_2$].[18]

Electrochemical Behaviour. [Pt_2Cl_2(pymS)$_4$] (**1**) exhibits an irreversible two-electron reduction process at −0.38 V and an irreversible two-electron oxidation process at 0.13 V in CH_2Cl_2 (Fig. 6). The bromo analogue also exhibits a similar cyclic voltammogram with somewhat more positive reduction (−0.24 V) and identical reoxidation potentials. The redox potentials are illustrated in Fig. 6 with those of analogous complexes [Pt_2X_2(pyt)$_4$] (X^- = Cl^-, Br^-; pyt = pyridine-2-thiolate)[4] and [Pt_2X_2(5-mpyt)$_4$] (X^- = Cl^-, Br^-; 5-mpyt = 5-methylpyridine-2-thiolate)[5] for comparison. Cyclic voltammograms of these complexes were newly measured under the same conditions as used for [Pt_2X_2(pymS)$_4$] measurements. Dinuclear Pt(III) complexes having quadruply bridged structure exhibit basically similar patterns of cyclic voltammograms in organic solvents. The Pt(III) species of the same bridging ligands are reduced at different reduction potentials depending on the different axial ligands. The oxidation potentials are practically the same, however. When the Pt(III) species are once reduced to the Pt(II) dimer, concomitant Pt–Pt and Pt-(axial ligand) bond cleavages occur, and thus they are re-oxidized at the same oxidation potential. In all complexes in Fig. 6, the reduction potentials of the Cl complexes are more negative than those of the Br analogues. This reflects the electronegativity of the axial ligands. The difference in the reduction potentials of Cl and Br complexes are slightly different depending on the bridging ligands (0.11 V for [Pt_2X_2(pymS)$_4$], 0.07 V for [Pt_2X_2(pyt)$_4$], 0.09 V for [Pt_2X_2(5-mpyt)$_4$]). The facts that

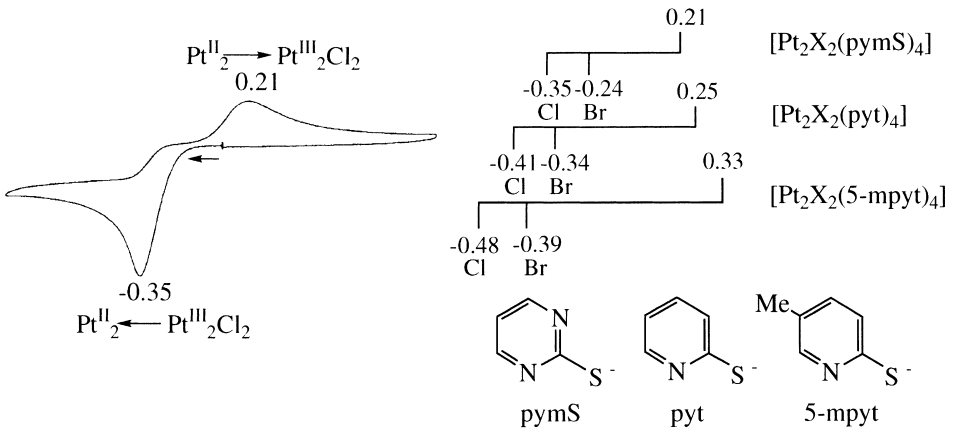

Fig. 6. Cyclic voltammogram of $[Pt_2Cl_2(pymS)_4]$ **1** in 0.1 M $TBAPF_6$-CH_2Cl_2 at a glassy-carbon electrode with a scan rate of 50 mV/s. The oxidation and reduction potentials of $[Pt_2X_2(pymS)_4]$ ($X^- = Cl^-$ (**1**), Br^- (**3**)) are also schematically illustrated with those of $[Pt_2X_2(pyt)_4]$ ($X^- = Cl^-$, Br^-) and $[Pt_2X_2(5\text{-}mpyt)_4]$ ($X^- = Cl^-$, Br^-).

the reduction potentials of $[Pt_2X_2(pymS)_4]$ are more positive than those of $[Pt_2X_2(pyt)_4]$ and $[Pt_2X_2(5\text{-}mpyt)_4]$ and that the oxidation potentials of the pymS complexes are more negative than those of the pyt and 5-mpyt complexes indicate that the pymS complexes are easier both to be reduced and to be oxidized than pyt and 5-mpyt complexes. In other words, electronic repulsion in $5d_{z^2}$ orbital in $[Pt_2(pymS)_4]$ is higher and the stability of Pt(III) oxidation state in $[Pt_2X_2(pymS)_4]$ is less than for pyt and 5-mpyt complexes.

Conclusion

The reaction of $K_2[PtCl_4]$ with pyrimidine-2-thiol (pymSH) has been studied systematically. It is now clear that the major isomer of $[Pt_2Cl_2(pymS)_4]$ is *cis*. Previously reported "*3,1*" isomer has turned out to be a minor product. On the contrary, the reaction of $K_2[PtCl_4]$ with 4-methylpyrimidine-2-thiol afforded a mixture of dinuclear Pt(III) complex, *cis*-$[Pt_2Cl_2(4\text{-}mpymS)_4]$, and mononuclear Pt(II) complex, *trans*-$[Pt(4\text{-}mpymS)_2]$. While the dinuclear Pt(III) complex is resistant toward oxidation, the mononuclear Pt(II) complex can be oxidized by Ce(IV) to give mononuclear Pt(IV) complex. When 4,6-dimethylpyrimidine-2-thiol is employed as a ligand, the mononuclear Pt(II) complex is the only product, due to steric hindrance. X-ray structural analyses of some of the complexes, and the electrochemical studies have revealed some characteristic features of the Pt complexes of pyrimidine-2-thiolate and its substituted ligands.

This work was supported by Grants-in-Aid for Scientific Research (Nos. 12023242 and 12640542) to KU from the Ministry of Education, Science, Sports and Culture.

References

1 K. Umakoshi and Y. Sasaki, *Adv. Inorg. Chem.*, **40**, 187 (1994).
2 R. Cini, F. P. Fanizzi, F. P. Intini, and G. Natile, *J. Am. Chem. Soc.*, **113**, 7805 (1991).
3 L. A. M. Baxter, G. A. Heath, R. G. Raptis, and A. C. Willis, *J. Am. Chem. Soc.*, **114**, 6944 (1992).
4 K. Umakoshi, I. Kinoshita, A. Ichimura, and S. Ooi, *Inorg. Chem.*, **26**, 3551 (1987).
5 K. Umakoshi and Y. Sasaki, *Inorg. Chem.*, **36**, 4296 (1997).
6 D. M. L. Goodgame, R. W. Rollins, and A. C. Skapski, *Inorg. Chim. Acta*, **83**, L11 (1984).
7 D. M. L. Goodgame, R. W. Rollins, A. M. Z. Slawin, D. J. Williams, and P. W. Zard, *Inorg. Chim. Acta*, **120**, 91 (1986).
8 D. M. L. Goodgame, A. M. Z. Slawin, D. J. Williams, and P. W. Zard, *Inorg. Chim. Acta*, **148**, 5 (1988).
9 A. C. T. North, D. C. Phillips, and F. S. Mathews, *Acta Crystallogr.*, **A24**, 351 (1968).
10 R. A. Jacobson, REQABS, Molecular Structure Corp., The Woodlands, TX (1998).
11 P. T. Beurskens, G. Admiraal, G. Beurskens, W. P. Bosman, R. de Gelder, R. Israel, and J. M. M. Smits, The DIRDIF94 Program System., Crystallography Laboratory, University of Nijmegen, The Netherlands (1994).
12 A. Altomare, G. Cascarano, C. Giacovazzo, A. Guagliardi, M. C. Burla, G. Polidori, and M. Camalli, *J. Appl. Crystallogr.*, **27**, 435 (1994).
13 C. J. Gilmore, MITHRIL-an integrated direct methods computer program, University of Glasgow, Scotland (1990).
14 teXsan: Crystal Structure Analysis Package, Molecular Structure Corporation, The Woodlands, TX 77381, USA (1999).
15 E. S. Raper, *Coord. Chem. Rev.*, **153**, 199 (1996).
16 J. Forniés, C. Fortuño, M. A. Gómez, B. Menjón, and E. Herdtweck, *Organometallics*, **12**, 4368 (1993).
17 R. D. Shannon, *Acta Crystallogr.*, **A32**, 751 (1976).
18 R. Fernández-Galán, B. R. Manzano, A. Otero, N. Poujaud, and M. Kubicki, *J. Organomet. Chem.*, **579**, 321 (1999).